

# Arctic Ocean gravity, geoid and sea-ice freeboard heights from ICESat and GRACE

R. Forsberg and H. Skourup

Geodynamics Department, Danish National Space Center, Copenhagen, Denmark

Received 6 June 2005; revised 10 August 2005; accepted 3 October 2005; published 4 November 2005.

[1] ICESat laser measurements provide a high-resolution mapping of the sea-ice surface of the Arctic Ocean, which can be inverted to determine gravity anomalies and sea-ice freeboard heights by a “lowest-level” filtering scheme. In this paper we use updated terrestrial gravity data from the Arctic Gravity Project in combination with GRACE gravity field models to derive an improved Arctic geoid model. This model is then used to convert ICESat measurements to sea-ice freeboard heights with a coarse lowest-level surface method. The derived freeboard heights show a good qualitative agreement to the coverage of multi-year sea-ice; however, comparison to an airborne lidar underflight north of Greenland shows that the lowest-level filtering scheme may introduce a bias. We finally use the ICESat and GRACE results to derive new gravity anomalies by Fourier inversion. The satellite-only gravity field shows all major tectonic features of the Arctic Ocean, and has an accuracy of 6 mGal compared to recent airborne gravity data, illustrating the usefulness of ICESat data for gravity field determination. **Citation:** Forsberg, R., and H. Skourup (2005), Arctic Ocean gravity, geoid and sea-ice freeboard heights from ICESat and GRACE, *Geophys. Res. Lett.*, 32, L21502, doi:10.1029/2005GL023711.

## 1. Introduction

[2] The measurement of sea-ice surface heights in the Arctic Ocean north of 81°N is made possible for the first time by the Geoscience Laser Altimeter System (GLAS) laser altimeter on board the Ice, Cloud and land Elevation Satellite (ICESat) [Zwally *et al.*, 2002]. In this paper we use ICESat data to derive a new satellite-only gravity field model of the Arctic Ocean, with preliminary sea-ice freeboard heights derived as an integral part of this work. The derived gravity and geoid models will support improved determination of sea-ice freeboard heights (and thus ice thickness), and improve earlier compilation of Arctic surface, airborne and satellite gravity models in the Arctic Gravity Project [Kenyon and Forsberg, 2001].

[3] The sea-ice freeboard height  $F$ , here including snow cover, may be expressed as:

$$F = h - N - \text{MDT} \quad (1)$$

where  $h$  is the ICESat tide-corrected ellipsoidal height estimate,  $N$  the geoid, and MDT the ocean mean dynamic topography. By assuming the MDT (and the errors in tidal models) to be predominantly of long-wavelength nature, the

MDT may be combined together with errors in  $h$  and  $N$  into a smooth along-track corrector signal  $\varepsilon$ , which may be estimated from laser data over leads with open water or thin ice. This principle works well for airborne laser altimetry [Hvidegaard and Forsberg, 2002], where  $\varepsilon$  is fitted to the “lowest levels” of the geoid-corrected altimetry ( $h - N$ ) by polynomial functions. In the case of GLAS, the larger laser footprint and along-track spacing ( $\sim 70$  m diameter and  $\sim 172$  m spacing) compared to airborne laser ( $\sim 1$  m across and along-track) will likely imply a larger distance between “tie” measurements over open water or thin-ice leads, thus making the lowest-level filtering scheme more uncertain. It is likely that use of ICESat surface reflectivity and waveform shape will improve the discrimination of ICESat measurements over open water or thin-ice leads; for a first detailed investigation of leads using ICESat data see Kwok *et al.* [2004]. In this paper we will use a relatively simple method for the lead lowest-level filtering, primary as an illustration of the potential of ICESat for free-board determination; our main focus of this paper will be on the geoid and gravity.

## 2. New Geoid Model of the Arctic From GRACE and ArcGP Compared to ICESat

[4] For sea-ice freeboard determination, geoid models may improve the lowest-level (or “lowest-surface”) filtering scheme, allowing longer distances between leads for the sea-level or thin-ice calibration levels [Hvidegaard and Forsberg, 2002]. Geoid models are derived by combining terrestrial gravity data with long-wavelength satellite gravity field models. With the recent improvements to gravity field models from Gravity Recovery and Climate Experiment (GRACE) satellite [Tapley *et al.*, 2004], current geoid accuracies at long wavelengths are extremely accurate (2–3 mm at 400 km wavelength). Remaining short-wavelength geoid inaccuracies are thus mainly due to inadequate coverage of high-resolution terrestrial gravity data.

[5] The Arctic Gravity Project has compiled a 5' gravity anomaly data grid for the Arctic region north of 64°N, based on all available surface, submarine and airborne gravity data, supplemented in some regions (mainly north of Siberia) with satellite altimeter-derived gravity [Laxon and McAdoo, 1998]. The typical grid resolution for regions with airborne gravity data is around 10' (18 km). For details of the project and data coverage see <http://earth-info.nga.mil/GandG/agp>.

[6] We generated a new geoid model of the Arctic region on a corresponding 5' grid using the GRACE GGM02S spherical harmonic model as a reference model (see <http://www.csr.utexas.edu/grace/gravity/ggm02>), using

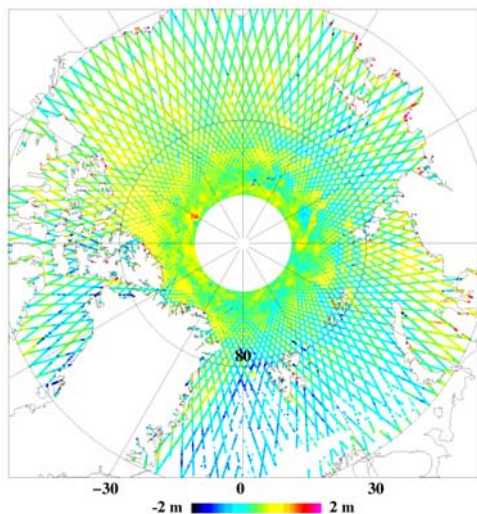


**Figure 1.** Difference between Arctic Geoid and ICESat sea-ice ellipsoidal heights, Feb. 21–Mar. 19, 2003 (Laser 1, Release 18).

an updated, yet unpublished ArcGP grid, incorporating new data sources, including new high-resolution data for Siberia. We used the “remove-restore” method, transforming the residual ArcGP gravity anomalies into geoid residuals by spherical FFT methods [Forsberg and Sideris, 1993]. The FFT methods implement Stokes’ formula

$$N = \frac{R}{4\pi\gamma} \iint \Delta g S'(\psi) d\sigma \quad (2)$$

where  $\Delta g$  is the gravity anomaly,  $R$  Earth radius,  $\gamma$  normal gravity, and  $\psi$  the spherical distance, with the integral in principle covering the whole earth. We used a modified Stokes’ function given by:

$$S'(\psi) = \sum_{l=n}^{\infty} \frac{2l+1}{l-1} w_l P_l(\cos \psi) \quad (3)$$

only allowing the short-wavelength gravity anomalies to affect the computed geoid at spectral bands higher than spherical harmonic  $n$ . We used a  $5'$  grid ( $10'$  in longitude), where spectral weights  $w_l$  were assigned to make a linear transition in the spherical harmonic band  $n = 100$  to  $n = 110$ , implying spherical harmonic data are used fully below harmonic degree 100, and terrestrial data fully above degree 110. To reduce edge effects, we extended the GRACE model by EGM96 to degree 360 by a linear blending scheme above degree 100.

[7] The new geoid represents a major improvement over the current ArcGP geoid, with changes of more than 1.5 m in some regions, primarily due to the inclusion of GGM02S. Figure 1 shows a comparison of the new geoid with ICESat sea-ice heights for the period February 21–March 19, 2003 (Laser 1; Release 18 GLA13 sea-ice records). If the geoid was perfect, and tidal errors and mean dynamic topography small, this plot would represent the freeboard heights  $F$ ; however, it is clear that residual track-related errors remain, likely in part due to ICESat saturation effects and inverse

barometer effects (no correction for these effects were applied due to our focus on geoid and gravity, and as the errors are to some degree reduced by our lowest-level filtering scheme). Localized geoid-related errors are clearly seen in Figure 1, notably at the location approx.  $85.5^\circ\text{N}$ ,  $120^\circ\text{W}$ , which corresponds to a data gap in ArcGP.

### 3. Approximate ICESat Sea-Ice Freeboard Heights

[8] For our sea-ice freeboard estimation we use here an experimental lowest-level filtering scheme, where a smooth surface is fitted by least-squares collocation to all ICESat track data for a particular period (Laser 1 and Laser 2a). We first selected the lowest values from the geoid-reduced ICESat data ( $h - N$ ) in cells of approximately 10 km size, using the new detailed geoid model outlined above, and these values were then gridded into a “lowest surface” using a smooth least-squares collocation estimator with a correlation length of 20 km and a priori data noise of 20 cm. Ideally this lowest surface would represent the sea-level surface, but we expect that in some heavy ice conditions this

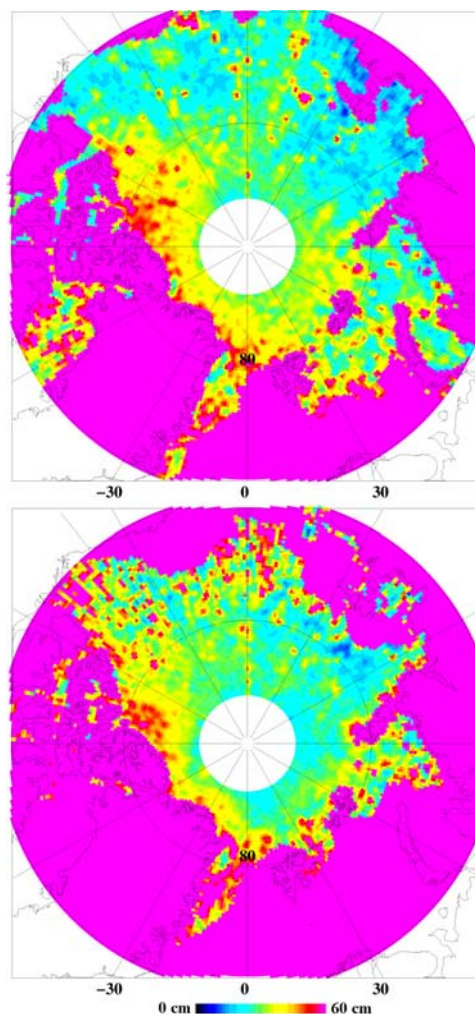


**Figure 2.** Sea-ice freeboard heights from ICESat for (top) Feb. 21–Mar. 19 2003 (Laser 1) and (bottom) Sep. 27–Nov. 28, 2003 (Laser 2a).

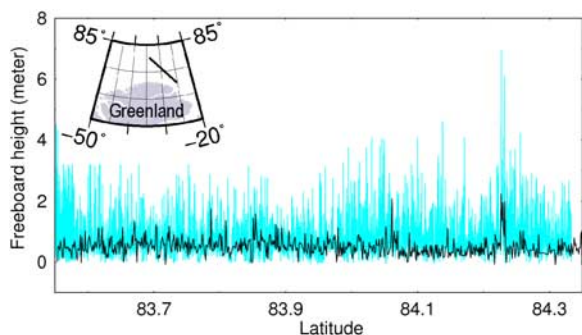


**Figure 3.** Example of a May 2004 flight north of Greenland, showing freeboard heights from airborne laser (blue) and ICESat (black; Laser 2b Release 19). The inset map shows location of track off northernmost Greenland.

surface does not correspond to open leads, but a mixture of thinner ice types, thus introducing a bias.

[9] The ICESat-derived freeboard estimates were subsequently Gaussian low-pass filtered at  $0.5^\circ$  resolution, after removing data in regions with less than 40% sea-ice concentration, derived from a combination of SeaWinds QuikSCAT backscatter and brightness temperatures [Ezraty and Piolle, 2001]. Figure 2 shows the freeboard height results for summer and winter periods 2003. It is seen that only the major overall ice features are revealed (like the thick ice north of Greenland and Ellesmere Island), and that seasonal thinning is apparent.

#### 4. A Comparison of ICESat Data to Airborne Lidar

[10] We compared our ICESat freeboard height results with high-resolution laser data from an airborne scanning lidar system mounted in a Twin-Otter [Forsberg et al., 2001]. The used airborne lidar system maps heights along a swath of 250 m width, with a laser resolution of approximately 1 m both across and along-track, and height accuracy of a few cm. The flight was carried out on May 25, 2004, off northern Greenland, within 8 hrs of an ICESat passage (no ice movement occurred during this period due to calm conditions, as verified by repeated ERS SAR imagery). Figure 3 shows a 80 km long coincident flight section, with ICESat freeboard heights and corresponding airborne freeboard heights (interpolated to the ICESat footprint locations from the dense swath laser coverage), using an along-track lowest level filtering scheme of resolution approx. 15 km. The airborne and ICESat freeboard heights show a good quantitative agreement, but due to lack of resolution ICESat underestimates narrow features such as the very large pressure ridges, as well as narrow leads. The latter results in an apparent bias of approximately 25 cm in the estimated lowest levels, indicating that ICESat with a coarse lowest-level filtering may underestimate sea-ice freeboard heights in regions of compact multi-year ice.

#### 5. ICESat-Derived Gravity Anomalies of the Arctic Ocean

[11] Removal of sea-ice freeboard heights from the ICESat-derived sea-ice heights will yield an approximation

to the geoid surface, neglecting the MDT. This geoid can be inverted into gravity anomalies using Fast Fourier Transform (FFT) techniques, equivalent to the derivation of marine gravity anomalies from satellite radar altimetry over the open oceans. In the present computations we take into account only long-wavelength freeboard heights, and use a Wiener filter method to suppress short-wavelength noise, in the Fourier domain expressed as

$$F(\Delta g) = G \frac{k}{1 + ck^4} F(N) \quad (4)$$

where  $F$  is the two-dimensional Fourier transform,  $k$  is the wave number, and  $c$  is a resolution constant [Forsberg and Solheim, 1988; Andersen and Knudsen, 1998]. We use (4) combined with a remove-restore technique keeping the GRACE information at longer wavelengths. This scheme reduce the effects of possible lowest-level biases, as well as suppresses the “leakage” of the ArcGP data used in the freeboard estimation into the final ICESat gravity product.

[12] The FFT gravity inversion was done using available 2003 ICESat data only (laser 1 and laser 2a, release 18). We

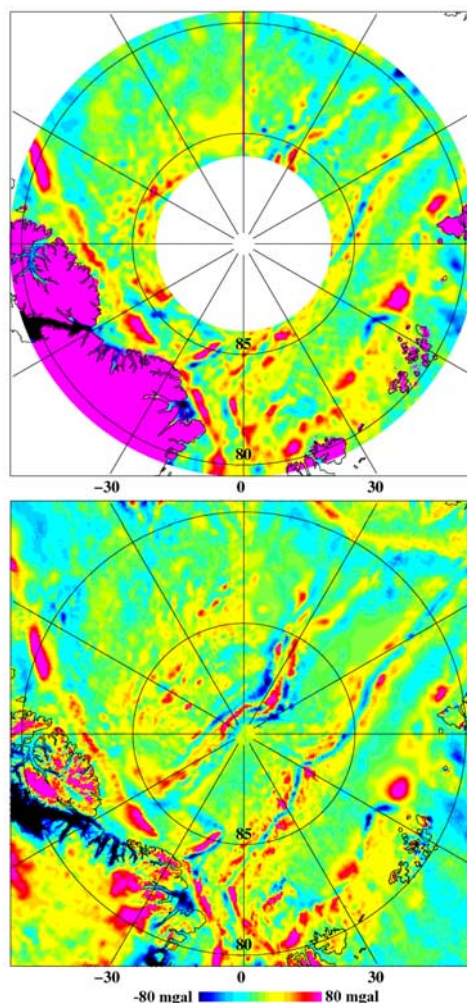


**Figure 4.** Gravity anomalies derived from ICESat and GRACE (upper) compared to the gravity anomalies of the Arctic Gravity Project (lower).

**Table 1.** ICESat-Derived Gravity Anomalies Compared to Recent Airborne Data North of Greenland and Svalbard (Unit: mGal)

Airborne Gravity Data Set	Original Data		ICESat Difference	
	Mean	Std. Dev.	Mean	Std. Dev.
US Naval Res. Lab. 1998–99 (83–86°N)	9.7	23.3	–1.3	6.4
KMS ESAG-2002 survey (84–86°N)	11.2	23.7	0.1	6.3

removed a bias of approximately 20 cm between laser 1 and 2a by a draping technique, and then performed the FFT computations in 4° bands with 2° overlaps in the latitude zone 79°–86°N (south of 79°N the available ICESat tracks are too widely separated to give accurate gravity). The composite GGM02S/EGM96 model was used as reference. We found that a Wiener filtering resolution of 20 km provided the best results.

[13] Figure 4 shows the gravity anomalies derived from (top) ICESat and GRACE compared to (bottom) the ArcGP data. The qualitative agreement between the data sets is quite stunning, with the ICESat data clearly showing major tectonic features such as the Lomonosov and Gakkell Ridges, as well as the continental shelf breaks. Comparisons to the ArcGP data and recent high-accuracy airborne gravity data (errors of 2 mGal r.m.s.) north of Greenland and Svalbard are shown in Table 1. We estimate that the accuracy of the ICESat gravity is around 6 mGal r.m.s., comparable to results of ERS radar altimetry in many open-ocean regions. It is anticipated that more ICESat data from later operating periods will improve the gravity accuracy even further, and contribute to improved ArcGP gravity and geoid grids. This is especially true for the eastern sector of the Arctic Ocean, where the original ArcGP grid was predominantly based on digitized Russian gravity maps of unknown underlying data density and ERS altimetry.

## 6. Conclusions

[14] We have used GRACE and ArcGP terrestrial gravity data to make an improved geoid of the Arctic Ocean, useful as a reference for sea-ice freeboard height mapping. Using a relatively simple lowest level filtering scheme, approximate freeboard height fields have been generated from ICESat data for the winter and fall 2003 periods, showing a general agreement with expected ice thickness distribution. Comparison to airborne lidar shows, however, that the ICESat freeboard estimates might be too low in regions of heavy ice cover. Using a GRACE reference field, the ICESat laser altimetry was used to recover free-air gravity anomalies

directly over the Arctic Ocean, giving a surprisingly good result (6 mGal r.m.s.) in spite of the relatively short data span, illustrating the exciting potential of ICESat and future satellites such as CryoSat for gravity field mapping.

[15] **Acknowledgments.** We thank NASA's ICESat Science Project and the NSIDC for distribution of the ICESat data, see <http://icesat.gsfc.nasa.gov> and <http://nsidc.org/data/icesat/>. We thank Donghui Yi for providing the May 25, 2004, ICESat data.

## References

- Andersen, O. B., and P. Knudsen (1998), Global marine gravity field from the ERS-1 and GEOSAT geodetic mission altimetry, *J. Geophys. Res.*, *103*, 8129–8137.
- Ezraty, R., and J. F. Piolle (2001), SeaWinds on QuikSCAT Polar Sea Ice Grids User Manual, *CONVECTION Rep. 5*, 29 pp., Eur. Comm., Brussels.
- Forsberg, R., and M. G. Sideris (1993), Geoid computations by the multi-band spherical FFT approach, *Manuscr. Geod.*, *18*, 82–90.
- Forsberg, R., and D. Solheim (1988), Performance of FFT methods in local gravity field modelling, paper presented at Chapman Conference on Progress in the Determination of the Earth's Gravity Field, AGU, Ft. Lauderdale.
- Forsberg, R., K. Keller, and S. M. Jacobsen (2001), Laser monitoring of ice elevations and sea-ice thickness in Greenland, *Int. Arch. Photogramm. Remote Sens. Spatial Inf. Syst.*, *XXXIV*, 163–169.
- Hvidegaard, S. M., and R. Forsberg (2002), Sea-ice thickness from airborne laser altimetry over the Arctic Ocean north of Greenland, *Geophys. Res. Lett.*, *29*(20), 1952, doi:10.1029/2001GL014474.
- Kenyon, S., and R. Forsberg (2001), Arctic Gravity Project—A status, in *Gravity, Geoid and Geodynamics 2000, International Association of Geodesy Symposia*, vol. 123, edited by M. G. Sideris, pp. 391–395, Springer, New York.
- Kwok, R., H. J. Zwally, and D. Yi (2004), ICESat observations of Arctic sea-ice: A first look, *Geophys. Res. Lett.*, *31*, L16401, doi:10.1029/2004GL020309.
- Laxon, S., and D. McAdoo (1998), Satellites provide new insights into polar geophysics, *Eos Trans. AGU*, *79*, 69–72.
- Tapley, D. B., S. Bettadpur, J. Ries, P. Thomson, and M. Watkins (2004), GRACE measurements of mass variability in the earth system, *Science*, *305*, 503–505, doi:10.1126/science.1099192.
- Zwally, H. J., et al. (2002), ICESat's laser measurements of polar ice, atmosphere, ocean and land, *J. Geodyn.*, *24*, 405–445.

R. Forsberg and H. Skourup, Geodynamics Department, Danish National Space Center, Juliane Maries Vej 30, DK-2100 Copenhagen O, Denmark. (rf@spacecenter.dk)